Journal of Biomedical Optics

BiomedicalOptics.SPIEDigitalLibrary.org

Optically-tracked handheld fluorescence imaging platform for monitoring skin response in the management of soft tissue sarcoma

Emilie Chamma
Jimmy Qiu
Liis Lindvere-Teene
Kristina M. Blackmore
Safa Majeed
Robert Weersink
Colleen I. Dickie
Anthony M. Griffin
Jay S. Wunder
Peter C. Ferguson
Ralph S. DaCosta

SPIE.

Optically-tracked handheld fluorescence imaging platform for monitoring skin response in the management of soft tissue sarcoma

Emilie Chamma,[a] Jimmy Qiu,[b] Liis Lindvere-Teene,[a] Kristina M. Blackmore,[a] Safa Majeed,[a] Robert Weersink,[a,b,c] Colleen I. Dickie,[b,d] Anthony M. Griffin,[e] Jay S. Wunder,[e,f] Peter C. Ferguson,[e,f] and Ralph S. DaCosta[a,c,g,*]
[a]University Health Network, Princess Margaret Cancer Centre, Toronto Medical Discovery Tower, MaRS Centre, 101 College Street, Toronto, Ontario M5G 1L7, Canada
[b]Princess Margaret Cancer Centre, Radiation Medicine Program, 610 University Avenue, Toronto M5G 2M9, Canada
[c]University Health Network, Techna Institute, 124-100 College Street, Toronto, Ontario M5G 1P5, Canada
[d]Princess Margaret Cancer Centre, Department of Radiation Oncology, 610 University Avenue, Toronto M5G 2M9, Canada
[e]Division of Orthopedic Surgery, Mount Sinai Hospital, 600 University Avenue, Toronto M5G 1X5, Canada
[f]Lunenfeld-Tanenbaum Research Institute, Mount Sinai Hospital, 600 University Avenue, Toronto M5G 1X5, Canada
[g]University of Toronto, Department of Medical Biophysics, Toronto Medical Discovery Tower, MaRS Centre, 101 College Street, Room 15-701, Toronto, Ontario M5G 1L7, Canada

Abstract. Standard clinical management of extremity soft tissue sarcomas includes surgery with radiation therapy. Wound complications (WCs) arising from treatment may occur due to bacterial infection and tissue breakdown. The ability to detect changes in these parameters during treatment may lead to earlier interventions that mitigate WCs. We describe the use of a new system composed of an autofluorescence imaging device and an optical three-dimensional tracking system to detect and coregister the presence of bacteria with radiation doses. The imaging device visualized erythema using white light and detected bacterial autofluorescence using 405-nm excitation light. Its position was tracked relative to the patient using IR reflective spheres and registration to the computed tomography coordinates. Image coregistration software was developed to spatially overlay radiation treatment plans and dose distributions on the white light and autofluorescence images of the surgical site. We describe the technology, its use in the operating room, and standard operating procedures, as well as demonstrate technical feasibility and safety intraoperatively. This new clinical tool may help identify patients at greater risk of developing WCs and investigate correlations between radiation dose, skin response, and changes in bacterial load as biomarkers associated with WCs. [DOI: 10.1117/1.JBO.20.7.076011]

Keywords: fluorescence imaging; optical tracking; radiation therapy; bacteria; sarcoma; surgery; wound complications.

Paper 150040R received Jan. 25, 2015; accepted for publication Jun. 25, 2015; published online Jul. 27, 2015.

1 Introduction

Both preoperative and postoperative external beam radiotherapy (RT) combined with limb salvage surgery have similarly high rates of local control in the management of extremity soft tissue sarcoma, regularly exceeding 90%.[1] Preoperative RT delivery is advantageous due to reduced volumes of tissues irradiated with a lower total prescribed dose compared to postoperative RT, leading to decreased late tissue morbidities, such as limb edema, joint stiffness, fractures, and fibrosis.[2,3] However, the main acute side effect associated with preoperative RT is wound complications (WCs). WCs are twice as frequent in patients receiving preoperative RT compared to postoperative RT (43 and 21%, respectively, for lower extremity tumors).[4] Furthermore, WCs still occur in ~30% of adult patients with lower extremity sarcomas despite tissue sparing preoperative intensity modulated radiation therapy (IMRT) combined with surgery.[5] Such wounds can be severe and often require repeated surgical procedures and/or deep wound packing followed by additional ongoing wound management, which reduces quality of life and increases health care costs.[6]

Currently, identifying sarcoma patients at risk of developing WCs remains challenging. Standard wound care for this population includes assessment of clinical signs and symptoms (skin erythema, heat, desquamation, and infection) by direct visual inspection under white light (WL) and by swabbing small skin areas for microbiological analysis in the laboratory, which may take approximately two to three days to provide a result.[7] However, this type of assessment is subjective, based on superficial signs of wound infection, and complicated for asymptomatic patients. Often, soft tissue sarcoma wound sites are challenging for clinical examination due to the large size of the surgical and/or irradiated region: for example, a nontargeted swab may lead to a false negative result in cases where infection is localized to a small area of a large wound. The importance of bacterial burden in wound assessment and care is well established.[8] During sarcoma treatment, biopsy, surgery, and RT can damage the skin at the surgical site, resulting in a microenvironment predisposed to bacterial colonization and infection. However, bacteria are occult under standard visualization of the skin. Thus, an imaging system capable of detecting bacteria during clinical examination may provide clinicians with important information about bacterial burden during sarcoma treatment.

*Address all correspondence to: Ralph S. DaCosta, E-mail: rdacosta@uhnresearch.ca

1083-3668/2015/$25.00 © 2015 SPIE

The ideal device would be handheld and easily integrated into the clinical workflow to spatiotemporally map bacterial load onto pre- and postoperative radiological images, as well as three-dimensional (3-D) IMRT dose plans. In this way, clinicians could rapidly assess patients at risk of developing WCs in an effort to prevent them. Early confirmation of clinically significant levels of bacteria at the treatment site, especially in asymptomatic patients, may enable care givers to obtain more useful microbiological samples and thus deliver optimum personalized care, which may ultimately result in fewer cases of infection and less severe WCs.

In this pilot clinical study, we demonstrate the technical and clinical feasibility of a new hybrid optically tracked imaging platform, equipped with a novel handheld fluorescence imaging device called portable real-time optical detection identification and guidance for intervention (PRODIGI), to detect the presence of bacteria in patients treated for sarcoma. Without the need for exogenous imaging agents, the multispectral imaging device can simultaneously detect collagen tissue and bacterial autofluorescence (AF) *in situ*, characterized by green and red AF signals, respectively, using violet-blue excitation light.[9] Various common species of pathogenic bacteria, such as *Staphylococcus aureus* and Diphtheroid bacilli, as well as heavy growth of commensal flora, can be detected using AF imaging. *In situ* bacterial AF can be attributed to endogenous porphyrins common to most bacterial species.[10–14] However, given the general commonality of endogenous fluorophores across bacteria species, AF imaging is unable to differentiate between bacteria species. The goals of this study were to establish feasibility of the imaging system and technical protocol for using the technology in the clinical setting, and to demonstrate that AF imaging of bacteria can be spatially and temporally coregistered with presurgical clinical computed tomography (CT) images and the IMRT dose distribution.

2 Material and Methods

2.1 *Portable Real-Time Optical Detection Identification and Guidance for Intervention Device*

The prototype PRODIGI fluorescence imaging device allows for handheld operation and combines multiband fluorescence emission filters and violet blue light-emitting diodes (LEDs) to enable both WL and AF imaging of tissues. It was validated for the detection and treatment guidance of chronic wound infection, in preclinical and clinical studies.[9,15] Briefly, the device consists of a low-cost consumer-grade sensor-based camera (Model DSC-T900, Sony) housed in a 3-D printed plastic body [Figs. 1(a) and 1(b)]. PRODIGI captures high-resolution 12.1 megapixel color images or 720p videos, which are displayed in real-time to the user in RGB format on a 3.5-in. touch-sensitive LCD screen. PRODIGI's illumination system consists of two violet-blue LEDs (405 nm, LedEngin LZ4-40UA10, emission 100 mW each for a total irradiance of 0.0044 W/cm^2 at a distance of 10 cm) and two excitation band pass filters (Thorlabs FB 400–40 nm). During AF imaging, a single dual-band fluorescence filter (Chroma 59022 m, $\lambda_{emission} = 500$ to 545 and 600 to 660 nm) housed in a slider is manually moved in front of the camera lens to block excitation light reflected from the tissue and to simultaneously allow the detection of AF from collagen and bacteria. AF images thus consist of green (collagen) and red (bacteria) signals only. PRODIGI is approved for use in clinical trials by Health Canada (ITA application #194991) and by University Health Network (UHN) institutional departments (Reusable Medical Device Committee, Medical Engineering Department).

2.2 *Optical Tracking System*

For this study, PRODIGI was combined with a commercial optical tracking system (OTS) (Polaris, NDI Medical, Waterloo, Ontario, Canada) to track the movement of the device in space relative to the patient over time. The OTS maps the patient in CT space relative to the RT dosimetric plan. This OTS addition consists of an infrared-light camera which tracks four IR reflective spheres (NDI Medical, Waterloo, Ontario, Canada) that are fixed to the external housing of the PRODIGI device [Fig. 1(a)].

The use of the OTS at University Health Network and Mount Sinai Hospital has been previously described.[16–20] Examples of CT-based navigation include guided pelvic osteotomy in sawbones and cadaver models,[20] localization of pulmonary nodules under bronchoscopy and fluorescence thoracoscopy in porcine models,[19] critical structure proximity alerts in skull base surgery and endoscopy,[18] and optical-CT fusion to improve superficial disease delineation.[16] CT-based navigation in soft tissue sarcoma is more challenging than other application sites due to soft tissue deformation from patient position differences in RT and surgery, changes in treated tissue throughout RT, and navigation off of historic planning CT due to lack of intraoperative CT in the standard of care. For this study, an infrared-light camera was installed in the treatment room, which enables six degrees of freedom (x, y, z, pitch, yaw, roll) measurements of the camera by localizing the attached IR reflective spheres. Software developed in-house registered and visualized the tracked camera pose relative to previously acquired radiological volumetric image data. In addition to registration, navigation, and covisualization (e.g., visual overlay) of multimodalities, the in-house software platform GTxEyes also performs camera calibration to remove camera distortion and calculates the sensor offset (translation and rotation) to camera center.[16,17] Radiation dose planning information can also be spatially coregistered and displayed on the real and virtual camera views as either isodose lines or colorwash using methods described previously by our group.[21] Viewing options using the GTxEyes software include orthogonal views through the CT image, corrected PRODIGI image, and a virtual 3-D CT rendered skin surface model viewed from the perspective of a virtual camera at the PRODIGI coordinates.

2.3 *Patient Population*

We enrolled 20 adult patients from the Princess Margaret Cancer Centre, University Health Network (Ontario, Canada) sarcoma clinic for treatment with preoperative external beam RT followed by surgical resection of lower limb soft-tissue sarcoma. This feasibility study was approved by UHN's Research Ethics Board (REB) and Mount Sinai Hospital's REB (11-1038, 12-0153-E, respectively). Informed consent was obtained according to institutional REBs requirements and good clinical practice (Ref. 22). Patients with pre-existing skin issues who received prior RT or required chemotherapy were ineligible for the study.

2.4 *Imaging Procedures*

At the RT planning stage, the planned surgical incision was drawn by the surgeon on the patient's skin and outlined with a flexible radiopaque wire at the time of the CT simulation

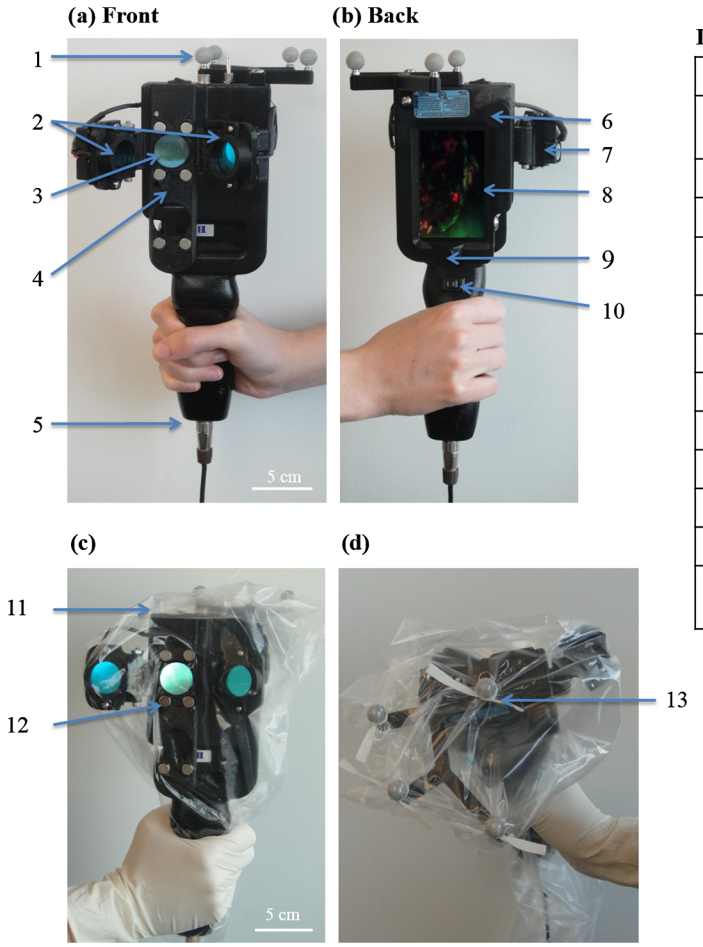

Legend

1	IR reflective spheres
2	Fluorescence 405 nm LEDs and excitation filters
3	Emission filter
4	Filter slide with magnets
5	Medical grade power supply
6	Filter slide mechanical pin
7	Heat sink with fans
8	Sony camera touch screen
9	Camera mechanical pin
10	On/off rocker switch
11	Sterile drape
12	Autoclaved magnets
13	Steri-strips tied around reflective spheres

Fig. 1 Photographs of different views of the handheld PRODIGI prototype device and its sterilization method. (a) The front view shows the main optical components, i.e., the four IR reflective spheres (1), the 405 nm fluorescence light-emitting diodes (LEDs) with excitation filters (2), the emission filter (3), and the filter slide with magnets (4) used for draping. The prototype is powered by a medical grade power supply (5). (b) The back view shows the mechanical pin to slide the emission filter in place during autofluorescence (AF) imaging (6), the heat sink and fans to cool down the LEDs (7) and the camera (8), and a mechanical pin (9) to keep it in place. The device is turned on/off by a rocker switch (10). (c) The device is fully covered by a sterile drape in order to perform intraoperative imaging (11). Four autoclaved magnets (12) keep the drape flush to prevent image quality degradation. (d) IR reflective spheres are used for tracking the device while in use, and steri-strips are tied around each sphere to ensure adequate tracking (13).

scan performed for RT treatment planning purposes [Fig. 2(a)]. This enabled localization of the entire future surgical scar on the 3-D CT rendered skin surface model. CT fiducial markers were also placed on the treatment setup points (small permanent tattoos). These tattoos and CT fiducial markers served as reference coordinates for registration of the PRODIGI and OTS systems in CT coordinates. A commercial extremity immobilization system was used for RT patient positioning.[23] Following CT simulation scan, an appropriate RT plan was designed as per institutional clinical standard guidelines.

Imaging was performed throughout sarcoma management [during RT, in the operating room [Figs. 2(b) and 2(c)] and at follow-up appointments]. Imaging was performed at three time points during RT: fractions 0, 12, and 25, i.e., at the beginning, middle, and end of the treatment. Four of the treatment setup points marked with radio-opaque fiduciary markers on the CT simulation scan were used to perform the optical and CT coregistration. An optically-tracked pointer tool using four IR reflective spheres (identical to those fixed to the PRODIGI device) was used to register the patient in space with respect to the IR camera. For this, the pointer was placed sequentially on each tattoo, identified, and spatially registered by the tracking IR camera and visualized in real-time on the CT scans using the software GTxEyes. The locations of the tattoos in the optical tracking coordinate system were then registered to the corresponding points in the CT image using the fiducial markers. Once registration was complete, the planned surgical scar was drawn on the patient's skin with a marker by superimposing the optically-tracked pointer on the scar visible on the CT scans. An imaging session consisted of both WL and corresponding AF imaging of the planned skin surgical incision and surrounding tissue. Room lights were turned off during AF imaging to avoid background signal and artifacts. The four reflective spheres on the PRODIGI device were pointed toward the IR camera to ensure proper 3-D tracking during the entire session.

The combined WL and AF images were part of a superset of data recorded using the tracking system. The superset also included preoperative patient CT and RT dose volumes. A skin

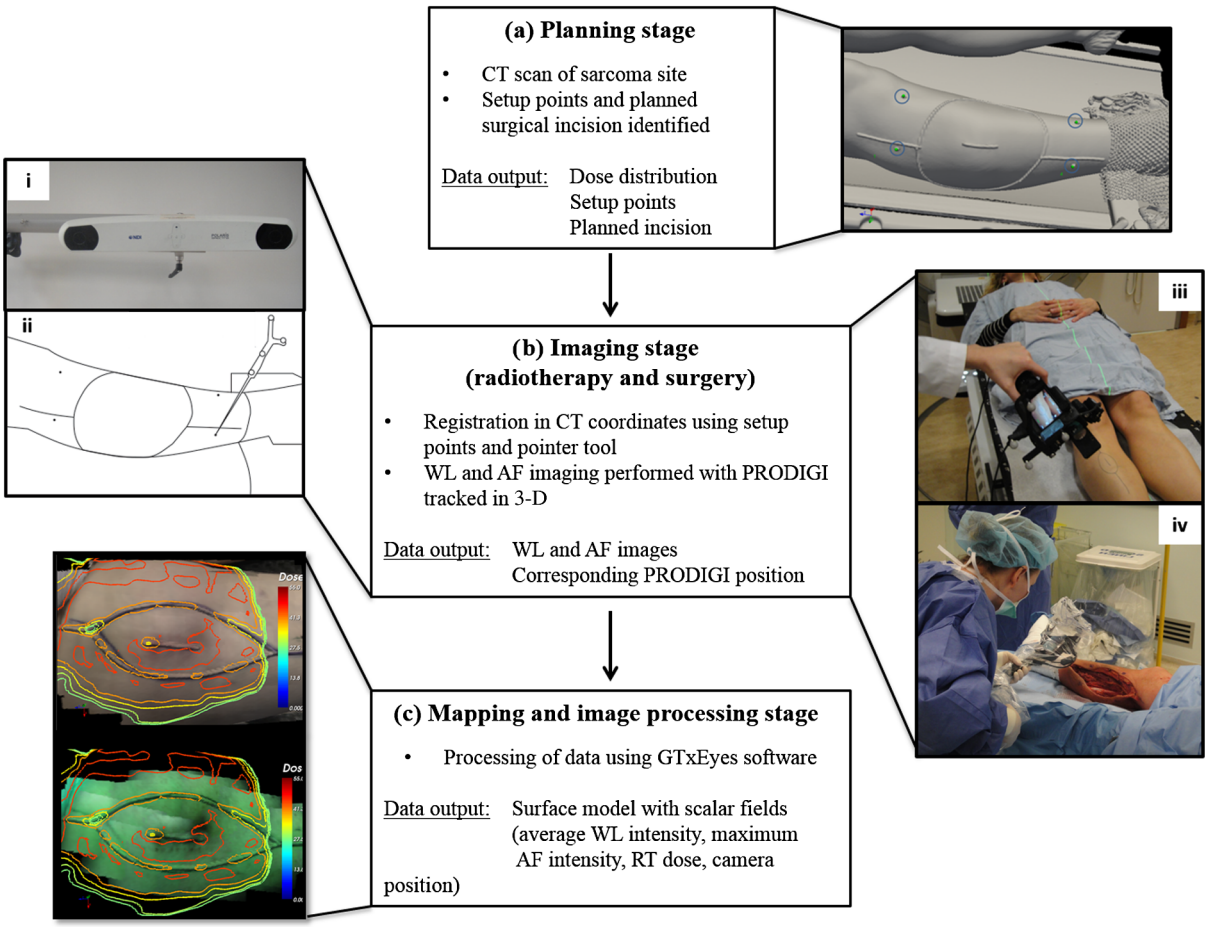

Fig. 2 Implementation workflow using the hybrid optically tracked PRODIGI imaging platform. (a) At the planning stage, a computed tomography (CT) scan of the sarcoma site was acquired and fiduciary markers were placed on the six treatment setup points (circled) and planned surgical scar. (b) The optical tracking system (i) and pointer tool (ii) were used to register the permanent tattoos in the CT coordinates and track the PRODIGI camera in space during white light (WL) and AF imaging. Imaging of the sarcoma site was performed during (iii) radiotherapy at fractions 0, 12, and 25 and (iv) during surgery. (c) The GtxEyes software creates a surface model from the CT scans and each WL and AF images are placed at matched camera pose. Each surface model point has the following scalar fields: average WL intensity, maximum AF intensity, and PRODIGI pose.

surface model was generated from the patient's CT, where each surface point held a quantitative tuple that contained RT dose, WL scalar, maximum intensity AF scalar, and camera pose corresponding to the AF scalar [Fig. 2(c)]. Overlay of WL and AF images on the 3-D CT rendered skin surface model was visualized and displayed using the open-source software ParaView (Fig. 3).

To perform imaging with the PRODIGI device in the operating room, a sterilization method was developed (and approved by the institutional Reusable Medical Device Committee) using a commercial grade sterile surgical drape (Cardinal Health Canada, Cat. #29-59029). The elongated drape was used to cover the entire PRODIGI device, including the camera unit and electrical power cord [Figs. 1(c) and 1(d)]. Six small circular neodymium magnets (Super Magnets, 8-mm diameter) were embedded into the slider holding the fluorescence emission filter and another six "complementary" magnets (autoclaved between uses in the operating room) were placed on the outside of the surgical drape to secure it and keep it flat relative to the camera sensor aperture, in order to minimize degradation of image quality. Steri-strips (3M Canada, Cat. #R1547) were applied on the outside of the draped device to secure the drape tightly around the IR reflective spheres in order to insure accurate tracking during imaging. To ensure that this method did not significantly affect the performance of the device, optical resolution was measured using a United States Air Force (USAF) 1951 resolution target consisting of horizontal and vertical lines that vary in size, thickness, and proximity. Clear antiseptic sponges (SoluPrep 3M Canada) were used to sterilize the surgical field in order to avoid the inherent AF signal from the red tint antiseptic normally used for sterilization. Imaging was performed at five time points: before and after sterilization of the surgical site (referred to as OR1 and OR2, respectively), once the surgical flap was raised (OR3), after tumor excision (OR4), and after surgical closure (OR5).

WL and AF imaging were performed on patients at multiple follow-up appointments without the OTS, since CT scans were no longer anatomically representative of the postoperative surgical site anatomy due to inherent deformation of the soft tissue shape and topography following surgery. Patients were tracked for a minimum of three months after surgery, or until closure of the surgical incision, to assess for WCs. A WC was defined as an

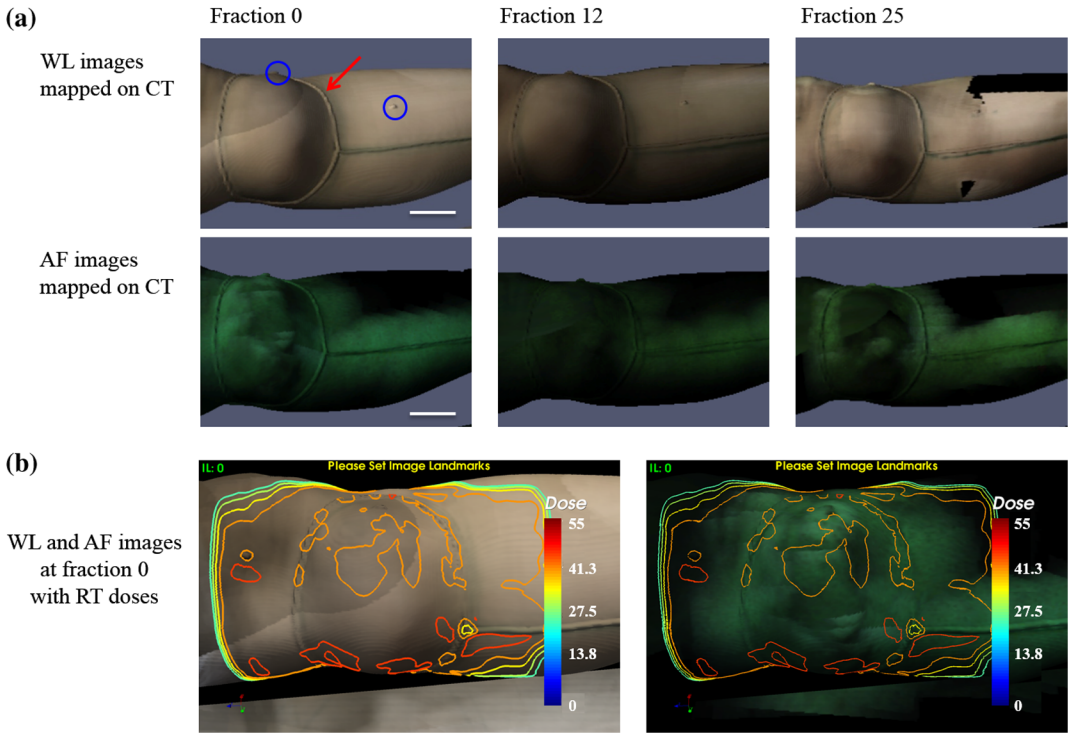

Fig. 3 Example of longitudinal WL and AF imaging of sarcoma treatment site during radiation therapy using the optically tracked PRODIGI imaging platform. (a) White light and corresponding AF images overlaid on three-dimensional (3-D) surface rendered CT scans for a sarcoma patient at fractions 0, 12, and 25. Software ParaView was used to visualize WL and fluorescence (FL) overlay. The planned surgical scar (red arrow) and irradiated area could be monitored longitudinally over the course of treatment. Visible fiducials are circled in blue. (b) Radiation doses in gray displayed in color isodose lines overlaid on CT scans with WL (left) and AF (right) imaging of the limb surface of the same patient. Scale bars: 5 cm.

unhealed surgical incision three months after surgery or as an incision requiring particular wound management, such as surgical debridement, antibiotics and/or vacuum therapy.

2.5 *Microbiology*

At each imaging session, swabbing of bacterial red AF positive and negative regions was performed to correlate with standard microbiological laboratory culture testing. Swab cultures were performed at Mount Sinai Hospital's microbiology department. Light growth of commensal flora was considered negative for the presence of pathogenic bacteria, whereas moderate to heavy growth of commensal flora and of other bacteria species were considered positive for the presence of pathogenic bacteria, and were deemed clinically relevant.[11]

2.6 *Statistical Analysis*

Diagnostic accuracy measures were calculated to determine the ability of the PRODIGI device to correctly identify the presence of pathogenic bacteria (as defined in Sec. 2.4). These measures included accuracy, positive predictive value (PPV), negative predictive value (NPV), and diagnostic odds ratio (DOR), a single indicator of test performance. Accuracy is defined as the number of true positive swabs (TP) plus the number of true negative swabs (TN) divided by the total number of swabs taken. The PPV (the probability that bacteria are present given positive AF) is defined by the number of TP swabs divided by the total number of TP and false positive (FP) swabs. The NPV (the probability that bacteria were not present given negative AF) is defined by the number of TN swabs divided by the total number of TN and false negative (FN) swabs. The DOR here is defined as the ratio of the odds of red AF when pathogenic bacteria is present relative to the odds of red AF when pathogenic bacteria is not present and is calculated by the following formula: $(\mathrm{TP}/\mathrm{FN}) \div (\mathrm{FP}/\mathrm{TN})$. The value of the DOR ranges from 0 to infinity with higher values indicating better discriminatory test performance.[24]

We also examined the clinical utility of PRODIGI to identify patients at risk for developing a WC post radiation treatment using logistic regression analysis to calculate the odds ratio (SAS version 9.4). Here we considered WC as the dependent variable, and AF measured using PRODIGI during radiation treatment (all three fractions combined) as the independent variable. Because some patients had multiple swabs taken at each fraction, we also adjusted for repeat swabs within a patient. Other variables considered as potential confounders for WC included: patient age, gender, ethnicity, tumor size, tumor location, and surgical flap thickness.

3 Results

WL and corresponding AF imaging could be performed longitudinally for patients with sarcoma during their complete treatment management process (including RT, intraoperatively and postoperatively) using the hybrid optically-tracked PRODIGI imaging platform. These imaging data could also be spatially-coregistered with preoperative radiological CT images of the

planned skin incision site in these patients [Fig. 4(a)] demonstrating technical feasibility of the approach.

3.1 *Longitudinal Imaging During Radiotherapy Treatments*

Clinically prescribed RT doses and dose distribution plans could be coregistered and overlaid for visualization of WL, AF, and CT images [Fig. 3(b)]. The clinically approved radiation dose distribution plan displayed on the skin surface images was the dose calculated at 1 mm for the evaluation of direct skin dose or at 3-mm below the skin surface to account for standard radiation dose build-up.[25] The accuracy of the registration and dose display was 4 ± 1.6 mm on average axially and laterally based on comparison of the fiducial markers and their corresponding skin tattoos on the patient. This error is due to a combination of soft tissue deformation, tumor changes following response to RT, and human variance when positioning the pointer on the skin tattoos. The imaging session added 10 min to the standard RT booking on fractions 0, 12, and 25.

3.2 *Intraoperative Imaging*

The optically-tracked PRODIGI platform was used to image the sarcoma site in the operating room to assess for the presence of bacteria at the surgical site. Imaging was performed quickly (10 min) without interference to the regular surgical workflow. Intraoperative WL and AF images taken before and after sterilization of the surgical site (OR1, OR2) were overlaid on the 3-D radiological CT scans to allow comparison to previous preoperative images of the same patient. However, overlay on the CT scans of WL and AF images taken after the surgical incision (OR3, OR4, OR5) were no longer spatially accurate due to tissue deformation at the surgical site.

Sterilization of the device using a commercial surgical drape did not interfere with the operation of the device (including optical tracking) nor did it significantly degrade WL and AF image quality. Indeed, the OTS's IR camera was able to effectively track the reflective spheres when the drape was fixed tightly around them. WL and AF imaging of a standard 1951 USAF resolution test target using PRODIGI with and without the surgical drape in place demonstrated image resolutions of 111.36 and 31.25 μm. Thus, the use of a surgical drape to ensure sterility of the device during OR use resulted in decreased spatial resolution of WL and AF images. However, this minimal loss of resolution did not adversely affect image quality or interpretation by the clinical user. The use of clear antiseptic sponges did not interfere with the detection of bacterial AF.

3.3 *Postoperative Imaging of Wound Complications*

Postoperative WL and AF imaging of the surgical site was performed at follow-up appointments using the PRODIGI device only (no OTS) to assess changes in bacterial burden and monitor healing. Postoperative imaging sessions ranged from 2 days to 10 months after surgery, with an average of four sessions per patient (range: 2 to 9). In total, nine patients (45%) developed WC following surgery. Logistic regression showed that patients who developed WC were almost three times more likely to have red AF regions during radiation treatment (all three fractions combined) compared to patients who did not develop WC (odds ratio = 2.76, 95% CI: 0.73, 10.48, $p = 0.14$), independent of other clinical risk factors.

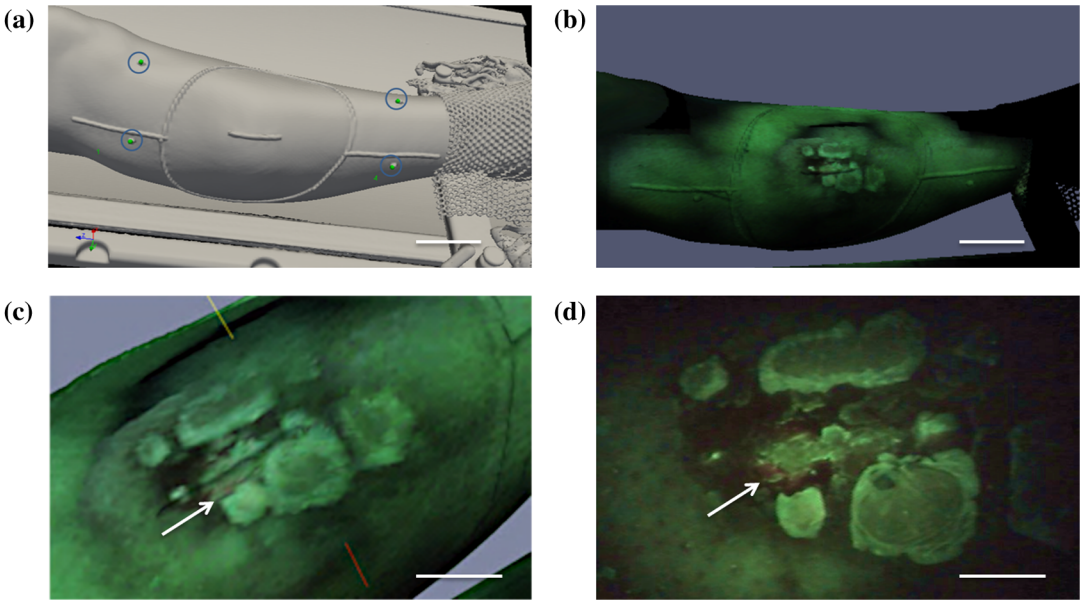

Fig. 4 Imaging of red fluorescent bacteria within surgical site at the radiotherapy stage. (a) CT rendering showing 3-D view of the soft tissue sarcoma site of the right leg of a patient—planned surgical incision and fiducials (circled). (b) Two-dimensional FL images of the skin surface at the surgical site skin were mapped on 3-D CT rendering of the extremity. (c) Magnified view of the surgical site in (b) showing the location and extent of red fluorescent bacteria between scabs, which appear bright green fluorescent due to high connective tissue content (arrow). (d) Corresponding original fluorescence image of the surgical site showing presence of red fluorescent bacteria (arrow). Red channel of the FL image was digitally enhanced for better visualization of this figure. Scale bars: (a) and (b) 5 cm, (c) and (d) 1 cm.

3.4 *Bacterial Autofluorescence*

Bacterial red AF signal was detected by the device in some patients during RT, in the operating room, and at follow-up appointments. At the RT stage, most patients experienced minor side effects from the radiation, such as mild erythema and dryness of the skin. Some patients ($n = 9$) had a pre-existing skin wound during the RT stage caused by a recent diagnostic biopsy that was not completely healed. Positive red fluorescence regions were discrete and found mostly around the wounds and biopsy scars or areas of severe skin erythema (Fig. 4). Imaging before sterilization of the surgical site showed the presence of bacterial red AF signal in three patients. After sterilization of the site, bacterial red AF was still detected in two of these patients, suggesting subsurface localization of bacteria. At follow-up appointments, discrete regions of laboratory culture-confirmed bacterial red AF signal were often found along the incision and surgical staples, while more extensive areas of bacterial red AF were found in patients with WCs.

Microbiological results from the swabbing of red AF positive and negative regions throughout the sarcoma treatment process confirmed the presence of pathogenic bacteria in red AF regions (Fig. 5). In total, 324 swabs were taken during the RT stage, in the operating room, and at follow-up appointments across all study participants. Bacterial species cultured from these swabs included *Staphylococcus aureus*, *Escherichia coli*, *Streptococcus*, Coliform bacilli, and commensal flora. The accuracy of the optically-tracked PRODIGI imaging platform to detect pathogenic bacteria was 85% (TP = 38, TN = 236). The PPV and NPV were 61% (TP = 38, FP = 24) and 90% (TN = 236, FN = 26), respectively. The DOR was 14.4 and was statistically significant (95% CI: 5.8 to 36.0, $p < 0.0001$).

4 Discussion

The hybrid optically-tracked imaging platform provided a new and useful method to assess bacterial presence and monitor skin response throughout the treatment management of patients with soft tissue sarcoma. The hand-held PRODIGI device could easily and rapidly perform WL and AF imaging of limbs in different clinical settings, i.e., in RT units, clinics, and surgical suites. The imaging platform integrated well into the clinical workflow of RT and operating rooms in which it was tested during our study. The OTS was easily installed and calibrated in these settings without interference of clinical workflow. Clinicians did not consider the need to turn off room lights briefly during AF imaging of the patient to be inconvenient in the study. Draping of the PRODIGI device for intraoperative use using a surgical drape caused minimal degradation in image resolution and did not interfere with the optical tracking of the device during operation. This minimal reduction of resolution did not adversely affect image quality or interpretation by clinical users.

Optical tracking of the device enabled the fusion of optical and CT modalities, where WL and AF images were superimposed over a patient's CT 3-D topographically-rendered surface model. Skin tattoos used for treatment were easy to locate and to register with the tracking system. No image artifacts due to movement after registration were found, given the use of a stereotactic mask to hold the limb in place. However, obtaining correct registration of the fiducial markers was difficult in situations where the position of the patient in the operating room was suboptimal. Position differences of the patient between RT and surgery can lead to darker AF images, deformations of the skin and soft tissue, and inaccessibility of registration fiducial markers. In

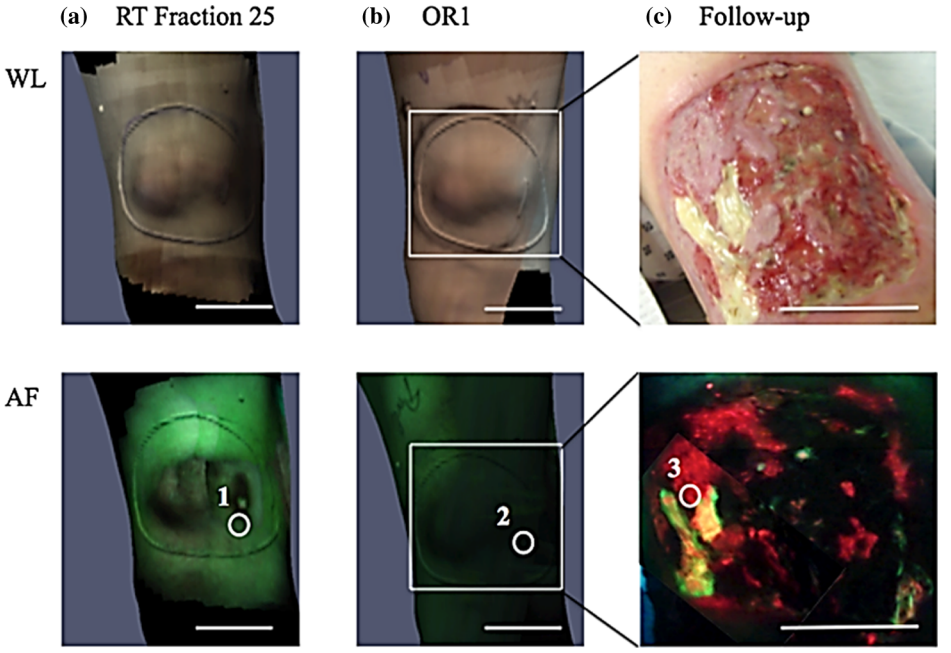

Fig. 5 WL and AF imaging throughout sarcoma management procedures and correlative swabbing for a patient with wound complication. (a) WL and AF images at radiotherapy fraction 25 show sarcoma site negative for bacterial red AF signal. Swab #1 confirmed presence of normal commensal flora only. (b) WL and AF images in the operating room before sterilization of the sarcoma site, negative for bacterial red AF signal. AF images are darker due to positioning of the patient. Swab #2 confirmed presence of normal commensal flora only. (c) WL and AF images at follow-up appointment show wound complication six weeks postoperation. Swab #3 taken in a positive red AF area confirmed heavy growth of G Streptococcus. Scale bars: 5 cm.

the case of inaccessible fiducials, either a subset of fiducials was used or additional anatomical landmarks were considered in consultation with the surgical team. The rigid registration accuracy of the skin tattoos was consistent throughout the RT sessions, with an error of 4 mm on average. This caused minimal variance in RT dose display and spatial AF signal correlation between imaging sessions.

The system illuminated the field of view with sufficient blue-violet light irradiance of 0.0044 W/cm^2 to detect both discrete and large areas of bacterial red AF. Few patients presented with bacteria at the beginning of their sarcoma management: those with nonhealed presurgical biopsy scars and severe skin erythema were more likely to present with bacterial red AF. In the operating room, three patients showed bacterial red AF signal at the surgical site. Standard sterilization of the skin surface with antiseptic sponges did not remove all of the bacteria in two of these patients based on fluorescence imaging and this was further confirmed by subsequent culture testing. For these patients, it is possible that bacteria beneath the skin surface were not eliminated by the sterilization procedure and the PRODIGI device could still detect them. Patients who later developed WCs presented with extensive areas of bacterial red AF at follow-up.

In this cohort of 20 patients, 9 (45%) developed WCs following surgery, which corroborates the numbers found in the literature when considering extremity limb sarcoma only.[4] Swabs taken from positive bacterial red AF regions revealed the presence of polymicrobial species that emitted red AF such as *Staphylococcus aureus* and *Escherichia coli*, common in both chronic and surgical wound infections.[26,27] Thus, AF imaging using this new platform could be used to assess different types of wounds. Visualizing these and other bacteria in real-time may improve wound care by guiding cleaning, sampling, and debridement of wounds in this patient setting. The relatively high accuracy (85%) and high DOR (14.4) of the imaging platform demonstrates its ability to correctly identify areas with and without bacterial AF in real-time due to moderate and heavy growth of pathogenic bacteria. In total, 26 false negatives were observed among all AF negative swabs ($n = 262$) accounting for the high NPV of the imaging platform (90%). In this study, the PPV was relatively low (61%) due to false positives that occurred in 24 of the total AF positive swabs ($n = 62$ AF positive areas) and because of the relatively low prevalence of bacteria in this population ($64/324 = 20\%$). In general, the lower the prevalence the lower the PPV and the higher the NPV as is demonstrated here.[28] Microbiological culture results for 15 (65%) of these false positive swabs showed light growth of commensal flora, considered negative here for the presence of pathogenic bacteria. However, in the case of sarcoma patients, wound location, possible skin erythema caused by external bean RT, and other host-related factors can potentiate the pathogenicity and growth of commensal flora leading to the development of WCs, since commensal flora can become pathogenic under certain conditions.[11] Future work will examine the possible effects of wound location and other factors (such as erythema and wound size) in order to improve the PPV of the imaging platform.

Overall, our results establish the technical feasibility of WL and AF imaging in the assessment of skin responses during complex management of sarcoma patients. These data also demonstrate that AF imaging may be a useful experimental tool for clinicians caring for cancer patients who may be prone to WCs following surgery and RT. Although statistical significance was not reached, likely as a result of our limited sample size, our initial data suggest that patients presenting with red AF during RT are nearly three times more likely to develop WC after surgery than patients not presenting with red AF during RT, independent of other clinical risk factors. These results warrant further investigation as they point to the potential utility of PRODIGI as a potential risk assessment tool during RT in this patient population. WL images can also enable the qualitative visual evaluation and monitoring of RT-induced skin reactions, e.g., erythema and desquamation, while AF images can map out the location and extent of bacteria that may influence wound healing. Overlay of WL and AF images, planned radiation treatment doses, and distribution on CT images can enable anatomical location-specific investigation of correlations between RT dose levels, erythema, presence of bacteria, and WCs. Progression of clinical signs and symptoms can be monitored and documented over time using spatio-temporal imaging provided by the platform. Overall, future applications of this technology may include clinicians using such information to study the role of external beam RT on skin damage and identify patients with moderate-to-heavy bacterial load who may have an increased risk for developing WCs, in order to adjust their treatment plan.

5 Conclusion

This paper is the first description of a new experimental imaging platform composed of a hand-held AF imaging device and optical-tracking system. We have demonstrated technical feasibility for serial multimodal image-based tracking of complex treatment in patients receiving management for extremity soft tissue sarcoma, with minimal disruption of clinical workflow during RT and in the intraoperative setting. The system is accurate in detecting clinically meaningful bacterial levels without the need for exogenous imaging agents and initial statistical analysis suggests there could be a correlation between bacterial autofluorescence during treatment and WCs following surgery. Further clinical investigations are underway at our institution using this technology, and will be the subject of a forthcoming publication.

Acknowledgments

This work was funded, in part, by Canadian Institutes of Health Research operating grant (CIHR MOP #93578), Ontario Centres of Excellence (MR60015-08), Health Technologies Exchange, Biodiscovery Toronto (project # BDT04-035-S3A), Canadian Institute for Photonic Innovation, Cancer Care Ontario Research Chair in Cancer Imaging to R.S.D., and by the Ontario Ministry of Health and Long Term Care. Partial support for R.W. is provided by the RACH Fund of the Princess Margaret Hospital Foundation. No funding for this project (including the experimental design, implementation of clinical trial, gathering, analysis, interpretation, publication, or editing of any data obtained from it) or salary support for R.S.D. was provided by the company for any part of the project from which this (or other referenced publication herein) is based.

Competing Financial Interests: RSD and his institution have a pending patent related to this work ("Device and method for fluorescence-based imaging and monitoring" USPTO WO 2009140757 A1), which is being commercialized. RSD is an independent investigator with a scientist appointment at the Princess Margaret Cancer Centre, University Health Network,

where he has been the principal investigator on this project. He is also a founder and a shareholder of a spin-off company commercializing the technology. He has board membership and receives compensation as chief scientific officer. At the time of this study, LLT was a part-time employee of the University Health Network (clinical associate). She also receives separate compensation as the clinical trials manager for the company, but her role in this project did not involve the company. No other authors are associated with or receive compensation or own shares of the company.

References

1. J. C. Yang et al., "Randomized prospective study of the benefit of adjuvant radiation therapy in the treatment of soft tissue sarcomas of the extremity," *J. Clin. Oncol.* **16**(1), 197–203 (1998).
2. A. M. Davis et al., "Function and health status outcomes in a randomized trial comparing preoperative and postoperative radiotherapy in extremity soft tissue sarcoma," *J. Clin. Oncol.* **20**(22), 4472–4477 (2002).
3. B. O'Sullivan et al., "Phase 2 study of preoperative image-guided intensity-modulated radiation therapy to reduce wound and combined modality morbidities in lower extremity soft tissue sarcoma," *Cancer* **119**(10), 1878–1884 (2013).
4. B. O'Sullivan et al., "Preoperative versus postoperative radiotherapy in soft-tissue sarcoma of the limbs: a randomised trial," *Lancet* **359**(9325), 2235–2241 (2002).
5. B. O'Sullivan et al., "Phase 2 study of preoperative image-guided intensity-modulated radiation therapy to reduce wound and combined modality morbidities in lower extremity soft tissue sarcoma," *Cancer* **119**(10), 1878–1884 (2013).
6. D. Schreiber et al., "Evaluating function and health related quality of life in patients treated for extremity soft tissue sarcoma," *Qual. Life Res.* **15**(9), 1439–1446 (2006).
7. P. R. Murray, "Manual approaches to rapid microbiology results," *Diagn. Microbiol Infect. Dis.* **3**(6 Suppl), 9S–14S (1985).
8. P. G. Bowler, "Wound pathophysiology, infection and therapeutic options," *Ann. Med.* **34**, 419–427 (2002).
9. Y. C. Wu et al., "Autofluorescence imaging device for real-time detection and tracking of pathogenic bacteria in a mouse skin wound model: preclinical feasibility studies," *J. Biomed. Opt.* **19**(8) 085002 (2014).
10. R. Richards-Kortum and E. Sevick-Muraca, "Quantitative optical spectroscopy for tissue diagnosis," *Annu. Rev. Phys. Chem.* **47**, 555–606 (1996).
11. P. G. Bowler and B. I. Duerden, "Wound microbiology and associated approaches to wound management," *Clin. Microbiol. Rev.* **14**, 244–269 (2001).
12. R. S. DaCosta, H. Andersson, and B. C. Wilson, "Molecular fluorescence excitation-emission matrices relevant to tissue spectroscopy," *Photochem. Photobiol.* **78**, 384–392 (2003).
13. B. Kjeldstad, T. Christensen, and A. Johnsson, "Porphyrin photosensitization of bacteria," *Adv. Exp. Med. Biol.* **193**, 155–159 (1985).
14. W. K. Philipp-Dormston and M. Doss, "Comparison of porphyrin and heme biosynthesis in various heterotrophic bacteria," *Enzyme* **16**, 57–64 (1973).
15. R. S. DaCosta et al., "Point-of-care autofluorescence imaging for real-time sampling and treatment guidance of bioburden in chronic wounds: first-in-human results," *PLoS One* **10**(3), e0116623 (2015).
16. R. A. Weersink et al., "Improving superficial target delineation in radiation therapy with endoscopic tracking and registration," *Med. Phys.* **38**(12), 6458–6468 (2011).
17. M. J. Daly et al., "Clinical implementation of intraoperative cone-beam CT in head and neck surgery," *Proc. SPIE* **7964**, 796426 (2011).
18. B. J. Dixon et al., "Augmented real-time navigation with critical structure proximity alerts for endoscopic skull base surgery," *Laryngoscope* **124**(4), 853–859 (2014).
19. T. Anayama et al., "Localization of pulmonary nodules using navigation bronchoscope and a near-infrared fluorescence thoracoscope," *Ann. Thorac. Surg.* **99**(1), 224–230 (2014).
20. A. Sternheim et al., "Navigated pelvic osteotomy and tumor resection: a study assessing the accuracy and reproducibility of resection planes in sawbones and cadavers," *J. Bone Joint Surg.* **97**(1), 40–46 (2015).
21. J. Qiu et al., "Displaying 3D radiation dose on endoscopic video for therapeutic assessment and surgical guidance," *Phys. Med. Biol.* **57**(20), 6601–6614 (2012).
22. R. DaCosta and P. Ferguson, "Evaluating bacterial response in sarcoma management using fluorescence imaging," https://clinicaltrials.gov/ct2/show/NCT02270086?term=NCT02270086&rank=1 (10 July 2015).
23. C. I. Dickie et al., "A device and procedure for immobilization of patients receiving limb-preserving radiotherapy for soft tissue sarcoma," *Med. Dosim.* **34**(3), 243–249 (2009).
24. A. S. Glas et al., "The diagnostic odds ratio: a single indicator of test performance," *J. Clin. Epidemiol.* **56**, 1129–1135 (2003).
25. F. M. Khan, *The Physics of Radiation Therapy*, 3rd ed., Lippincott Williams and Wilkins, Philadelphia, Pennsylvania 2003.
26. K. Gjødsbøl et al., "Multiple bacterial species reside in chronic wounds: a longitudinal study," *Int. Wound J.* **3**(3), 225–231 (2006).
27. A. Giacometti et al., "Epidemiology and microbiology of surgical wound infections," *J. Clin. Microbiol.* **38**(2), 918–922 (2000).
28. J. N. Mandrekar and S. J. Mandrekar, "Statistical methods in diagnostic medicine using SAS software," April 2005, http://www2.sas.com/proceedings/sugi30/211-30.pdf (29 June 2015).

Emilie Chamma is a clinical research coordinator at the Princess Margaret Cancer Centre, University Health Network, Toronto, Ontario. She obtained her MSc degree in biophotonics from Universite Laval in Quebec City, Quebec.

Jimmy Qiu is a research associate in the Radiation Medicine Program at Princess Margaret Cancer Centre, University Health Network.

Liis Lindvere-Teene is a clinical research coordinator at the Princess Margaret Cancer Centre, University Health Network. She obtained her MSc degree in medical biophysics at the University of Toronto in Toronto, Ontario.

Kristina M. Blackmore is a research associate at the Princess Margaret Cancer Centre, University Health Network. She obtained her MSc degree in biological anthropology from McMaster University in Hamilton, Ontario, and has completed graduate level courses in biostatistics and epidemiology as part of the MHSc in Community Health and Epidemiology at the University of Toronto, Ontario.

Safa Majeed is a summer student intern in the DaCosta lab, and an undergraduate student in life sciences at Queen's University in Kingston, Ontario. During her internship in the DaCosta lab, she participated in the preclinical and clinical trial research involving a variety of cancer imaging technologies, enriching her understanding of the scientific process and medical innovation.

Robert Weersink is a medical physicist in the Radiation Medicine Program at Princess Margaret Cancer Centre, University Health Network.

Colleen I. Dickie is a research radiation therapist in the Radiation Medicine Program at Princess Margaret Cancer Centre, University Health Network.

Anthony M. Griffin is a clinical research manager in the division of orthopedics surgery at Mount Sinai Hospital, Toronto, Ontario.

Jay S. Wunder is an orthopedic surgeon and surgeon-in-chief at Mount Sinai Hospital.

Peter C. Ferguson is an orthopedic surgeon at Mount Sinai Hospital and the program director in orthopedic surgery at the University of Toronto.

Ralph S. DaCosta holds the Cancer Care Ontario Chair in Cancer Imaging and is a scientist at the Princess Margaret Cancer Centre and Techna Institute at the University Health Network, where he leads a translationally-driven molecular imaging cancer research program.